

## Observation of dissipation asymmetries in tunnel junctions at high bias

A. F. Hebard

Bell Laboratories, Murray Hill, New Jersey 07974

(Received 2 July 1975)

When a metal-insulator-metal tunnel junction is biased at a potential which is a significant fraction of the total barrier height, there is an appreciable difference in the energies dissipated due to the relaxation on the one hand of the hot electrons created in the positive electrode and on the other hand of the relatively cooler hole excitations created in the negative electrode. This asymmetry has been observed in Al-I-Pb tunnel junctions immersed in liquid helium and 1°K and some simple ideas about energy flow and barrier parameters for these thin-film geometries have been quantitatively verified.

### I. INTRODUCTION

The phenomenon of tunneling between two metals separated by a thin ( $\sim 15\text{--}30 \text{ \AA}$ ) insulating barrier is relatively well understood from both a theoretical and experimental point of view.<sup>1-6</sup> For the case in which the voltage bias  $V$  is a significant fraction of the total barrier height, the favored tunneling processes are those which transfer an electron from close to the Fermi level  $E_F$  of the negatively biased electrode across the barrier at constant energy to an energy  $E \leq V$  with respect to  $E_F$  of the positive electrode. For each transfer of an electron across the barrier into the positive electrode there is a resulting hole excitation created in the negative electrode. These electrons and holes then relax by phonon emission to the Fermi levels of the respective electrodes. Because of the low thermal resistance across the tunnel barrier, the final steady-state temperature of the tunneling sandwich is the same for both electrodes and is determined primarily by the energy flows through the combined thermal conductances of each electrode to the outside environment.

We report here the observation of dissipation asymmetries in Al-I-Pb thin-film tunnel junctions immersed at 1°K in liquid helium. The effect is observable because there is an asymmetry in the electron and hole dissipations inherent to the tunneling process at high bias and the escape rate into the helium of the phonons created in the Pb electrode is greater than the escape rate into the helium of the phonons created in the Al electrode. It is further shown that a straightforward application of the independent particle tunneling equations explains in a *qualitative* way the dependence of this asymmetry on bias voltage; and helps to verify in a *quantitative* way some *ad hoc* assumptions about barrier parameters and energy flow in thin-film geometries.

### II. EXPERIMENTAL DETAILS

The experimental configuration is that of a thin film Al-I-Pb generator separated and insulated from a thin film Al-I-Al detector as depicted in the schematic cross section of Fig. 1(a). The films (1500 Å) were vacuum evaporated from resistive heaters at  $5 \times 10^{-7}$  Torr, and thermally grown Al oxide formed the tunneling barrier for both junctions. The SiO insulation was of the order of 1000 Å thick. The area common to both electrodes of the generator junction (1.63 mm<sup>2</sup>) overlapped the smaller area (0.28 mm<sup>2</sup>) of the detector junction. In order to facilitate the making of electrical connections, the junctions were evaporated as perpendicular cross strips with the detector leads rotated 45° with respect to the generator leads.

In Fig. 2 we plot as solid curves the energy dissipated ( $IV$ ) for both biases as a function of bias current. The different solid curves arise because there is a well-known intrinsic barrier asymmetry<sup>4-7</sup> in the Al-I-Pb tunneling barrier which manifests itself in an asymmetric current-voltage ( $I$ - $V$ ) characteristic. The barrier asymmetry is such [Fig. 1(b)] that the tunneling current is less for the Al<sup>-</sup> bias than it is for the same Al<sup>+</sup> bias. The dashed lines of Fig. 2 connect the points where the dissipation  $U^-$  in the generator junction with the Al electrode biased negatively (Al<sup>-</sup>) produces the same change in the detector as the corresponding dissipation  $U^+$  with the Al electrode biased positively (Al<sup>+</sup>). The detector junction was essentially used as a thermometer which was read out by electronically monitoring the temperature sensitive differential conductance as a function of voltage in the gap region. These dashed lines are hereafter referred to as *connectors*. One should note that the connectors are more or less vertical and parallel when the dissipation is plotted against current. The asymmetry increases

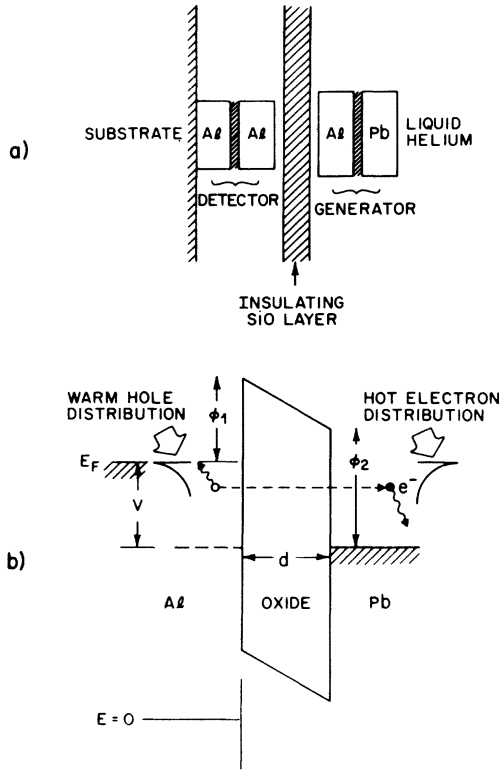


FIG. 1. (a) Schematic cross section of thin-film generator-detector configuration. (b) Schematic of asymmetric trapezoidal tunneling barrier at bias  $V$ .

with current (and voltage) to where, for example, the  $Al^-$  dissipation of

$$(1.25 \text{ V})(0.747 \text{ mA})/(1.63 \text{ mm}^2) = 0.57 \text{ mW/mm}^2$$

is 54% greater than the  $Al^+$  dissipation of

$$(0.835 \text{ V})(0.722 \text{ mA})/(1.63 \text{ mm}^2) = 0.37 \text{ mW/mm}^2.$$

The thermometric use of the detector junction was experimentally validated by the observation that the detector response as a function of detector voltage was identical for both of the generator dissipations defining a given connector. Furthermore, in the region of our measurements, there was no discernible difference between these response curves and the response obtained by simply warming the helium bath (with the generator current set at zero) to an appropriately higher temperature.

The importance of the Kapitza conductance between the Pb film and the helium is shown in the data on the right-hand side of Fig. 2. Here the same tunnel-junction configuration was taken up to room temperature and a 1000-Å SiO film was evaporated over the structure. The  $I$ - $V$  characteristics of both the generator and detector junctions changed only by a few percent during this

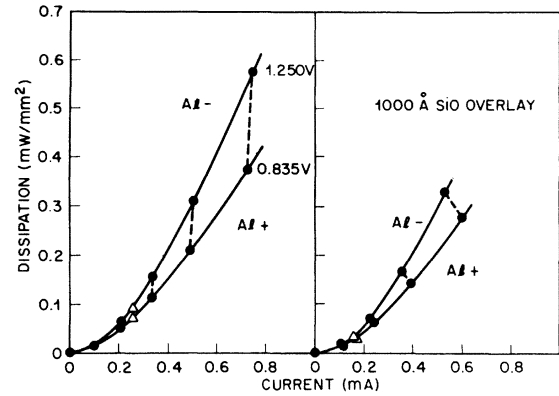


FIG. 2. Generator dissipation vs generator current showing connectors (dashed) both before and after 1000-Å SiO overlay.

procedure. The resulting connectors are now more nearly parallel with the current axis which implies that the dissipation is becoming more nearly symmetric as the Kapitza conductance to the helium is reduced. This was experimentally carried one step further by pumping away the liquid helium so that the sample was sitting only in exchange gas. The connectors then became exactly parallel to the current axis (symmetric dissipation) because all phonons were reflected from the interface towards the detector and all phonon energy generated by the relaxation processes (from both electrodes) were constrained to pass through the detector.

### III. TUNNELING DISSIPATION ASYMMETRY

We preface the analysis of these data by using the independent particle tunneling equations to calculate the asymmetries in the hot-carrier dissipations generated in the tunneling process. We assume for our model calculation an asymmetric trapezoidal barrier of the form  $\phi(x) = \phi_1 + E_F + x(\phi_2 - \phi_1 - V)/d$  [Fig. 1(b)].  $\phi_1$  ( $\phi_2$ ) is the barrier height on the Al (Pb) side and  $x$  is the tunneling direction measured from the Al electrode. Following Duke,<sup>3</sup> the tunneling current from left to right  $j_{LR}$  can be written

$$j_{LR} = \frac{4\pi m e}{h^3} \int dE_x D(E_x) \int dE_{\parallel} f(E) [1 - f(E + eV)],$$

which at 0°K ( $j_{RL} = 0$ ) reduces to

$$j = \frac{4\pi m e}{h^3} \left( eV \int_0^{E_F - eV} D(E_x) dE_x + \int_{E_F - eV}^{E_F} (E_F - E_x) D(E_x) dE_x \right), \quad (1)$$

where  $f(E)$  is the Fermi function,  $E$  is the total en-

ergy consisting of the sum of a component perpendicular to the barrier  $E_x$  and a parallel component  $E_{\parallel}$ , and

$$D(E_x) = \exp\left(\frac{-2(2m)^{1/2}}{\hbar} \int_0^d [\phi(x) - E_x]^{1/2} dx\right) \quad (2)$$

$$U_e = \frac{4\pi m}{h^3} \int dE_x D(E_x) \int dE_{\parallel} f(E) [1 - f(E + eV)] (E - E_F + eV) \\ = \frac{4\pi m}{h^3} \left[ \frac{(eV)^2}{2} \int_0^{E_F - eV} D(E_x) dE_x + \int_{E_F - eV}^{E_F} \left( \frac{E_F - E_x}{2} \right) (E_x - E_F + 2eV) D(E_x) dE_x \right]. \quad (3)$$

The corresponding expression for the hole dissipation  $U_h$  is similar but involves a different energy factor  $E_F - E$ . It is clear that the sum ( $U_e + U_h$ ) of the electron and hole dissipations must equal the total dissipation  $jV$ . This is physically transparent when we consider the transfer of a single electron across the barrier as in Fig. 1(b). This transfer leaves a hole a distance in energy units of  $E_F - E$  from  $E_F$  of the negatively biased electrode and an electron a distance  $E - E_F + eV$  from  $E_F$  of the positive electrode. The sum of these quantities is  $eV$ , which, from the point of view of the battery, is the potential drop experienced when supplying an electron at the Fermi level of the negative electrode and removing it from the Fermi level of the positive electrode.

Since electrons and holes are in some sense equivalent excitations, we should also consider the process<sup>8</sup> in which a hole tunnels from the sea of fully occupied holes above the Fermi level of the positive electrode into the electron sea (unoccupied holes) of the negative electrode. Here the favored tunneling processes are those which transfer holes from near the Fermi level of the positive electrode (leaving warm electrons) across the barrier at constant energy into the negative electrode where they appear as "hot" holes. The energy barrier to this hole transfer is measured in a negative direction to the top of the valence band of the insulator. Since the Fermi level of the Al is closer ( $\approx 2$  V) to the bottom of the conduction band of the oxide than it is to the top of the valence band (band gap is  $\sim 7-8$  V), the effective barrier to hole transfer is significantly greater than the barrier to electron transfer; thus resulting in a negligible contribution to the total current. If the Fermi levels were located symmetrically in the gap and if the electron and hole processes were equally probable, then the dissipation would be symmetric in both electrodes.

Numerical solutions to the above expressions have been obtained for the barrier parameters

is the WKB tunneling probability of an electron with energy  $E_x$  tunneling through a barrier of height and shape  $\phi(x)$ . To calculate the energy dissipation  $U_e$  associated with the injected hot-electron distribution, we sum over the energies each injected electron loses in relaxing to the Fermi level  $E_F$ , that is,

$d = 16 \text{ \AA}$ ,  $\phi_1 = 1.70 \text{ eV}$  and  $\phi_2 = 3.13 \text{ eV}$  and are summarized in Figs. 3-5. This value of  $\phi_1$  is in rough agreement with existing<sup>9,10</sup> determinations and  $d$  and  $\phi_2$  were picked somewhat arbitrarily to give a zero voltage conductance equal to the experimental value of  $2.63 \text{ } \Omega \text{ cm}^{-2}$ . No serious effort was expended in trying to independently measure these barrier parameters because previous work-

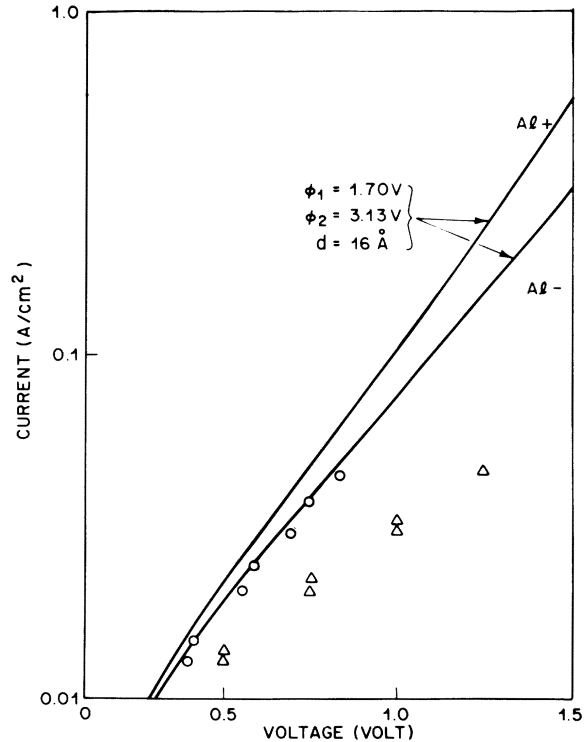


FIG. 3. Model calculation of current-voltage characteristics. For comparison, representative experimentally determined points corresponding to the solid circles of Fig. 2 are shown as open circles ( $\text{Al}^+$ ) and triangles ( $\text{Al}^-$ ). The scatter is caused by the slight change in junction characteristics which occurred during the warmup to room temperature for the  $\text{SiO}_2$  deposition.

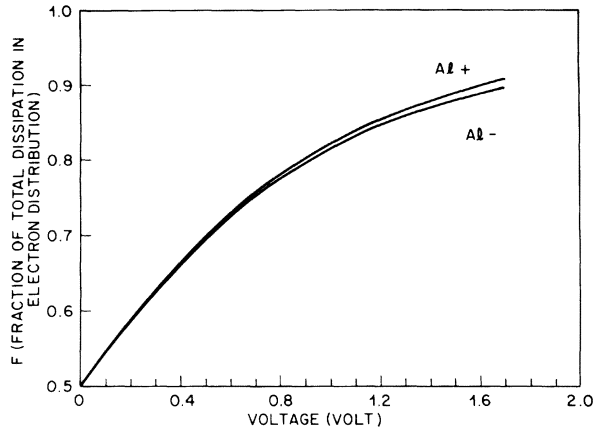


FIG. 4. Model calculation of fraction ( $F$ ) of total dissipation appearing in the electron distribution plotted against voltage.

ers<sup>7</sup> have found that the highly asymmetric conductance of Al-I-Pb junctions cannot be satisfactorily explained by the simple tunneling theories. For our present purposes, however, the qualitative features of the asymmetric trapezoidal barrier calculation are sufficiently illuminating to give a hint of the assumptions needed for a more quantitative analysis of the data. The salient fact here is that the fraction  $F = U_e/jV$  of the total energy in the hot-electron distribution as shown in Fig. 4 is approximately linear in voltage up to  $\sim 0.75$  V and at higher voltage is not very sensitive to bias polarity as are, for example, the  $I$ - $V$  curves of Fig. 3. It should be noted that, in this physically reasonable model calculation, as much as 90% of the total energy to be dissipated at a bias of only 1.6 V appears in the hot electron distribution.

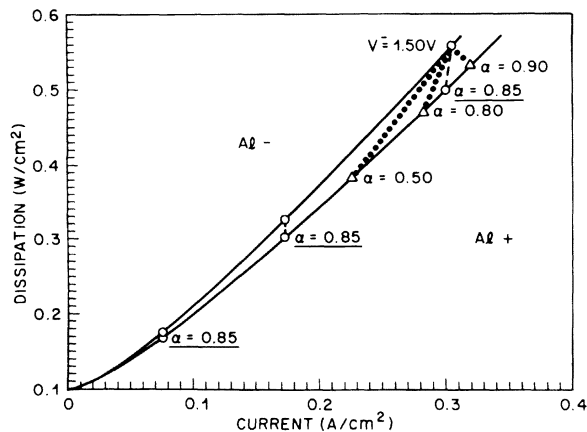


FIG. 5. Model calculation of generator dissipation vs generator current with connectors shown for different values of  $\alpha$ .

#### IV. PHONON FLOWS

Up to this point, we have sidestepped the question of how to treat the phonon distributions which result from the relaxation of the hot carriers. We start by defining  $f_{Al}$  ( $f_{Pb}$ ) as the fraction of energy resulting from hot carrier dissipation in Al (Pb) that gets to the detector in the form of phonons. The remainder goes out into the helium while a negligible amount is lost out the thin-film leads. Experimentally, the end points of the connectors of Fig. 2 are determined by the measured total dissipations  $U^- (=jV^-)$  and  $U^+ (=jV^+)$  which give an equivalent change in the detector. We are now able to write  $\mathcal{F}^- = (f_{Al}U_h^- + f_{Pb}U_e^-)/U^-$  [ $\mathcal{F}^+ = (f_{Al}U_e^+ + f_{Pb}U_h^+)/U^+$ ] as the fraction of the total dissipation  $U^-$  ( $U^+$ ) arriving at the detector and  $1 - \mathcal{F}^-$  ( $1 - \mathcal{F}^+$ ) as the fraction escaping into the helium. The coordinates of the connector end points are defined by the relation  $\mathcal{F}^-U^- = \mathcal{F}^+U^+$  or

$$f_{Al}U_h^- + f_{Pb}U_e^- = f_{Al}U_e^+ + f_{Pb}U_h^+. \quad (4)$$

This expression takes into account the phonon fluxes resulting from both the electron and hole dissipations at each bias. It should be noted that the equilibrium phonon distribution ("temperature") in the generator junction is assumed to be the same at each end of a connector.

Our *first hypothesis* is that  $f_{Al}$  and  $f_{Pb}$  can be written as constants independent of the bias voltage. That this is not an unreasonable assumption arises from the fact that the comparatively low-energy phonons which arrive at the detector or escape into the helium have energies small ( $\sim$ meV) compared to the dominant energies of their parent hot carriers ( $\geq 100$  meV). In summary, the hot carriers lose energy in a multistep process by emitting phonons which correspond predominantly to peaks in the phonon density of states. These high-energy phonons have short mean-free paths and immediately break pairs in the superconducting electrodes thus creating quasiparticles which relax to the high density-of-states gap edge. Recombination phonons of energy  $2\Delta$  are emitted as these excess quasiparticles at the gap edge recombine to form paired electrons. It is these recombination phonons which are an important component<sup>11,12</sup> of the phonon spectrum and hence play a pivotal role in determining the flow of energy into the helium.

Equation (4) can be rewritten in terms of the total energies as

$$U^+[(1 - \alpha)F^+ + \alpha] = U^-[1 - (1 - \alpha)F^-], \quad (5)$$

where  $\alpha = f_{Pb}/f_{Al} \leq 1$  and we have used the relations  $U_h^- = (1 - F^-)U^-$ ,  $U_e^- = F^-U^-$ , etc. Note that in the limit  $\alpha \rightarrow 1$  ( $f_{Pb} = f_{Al}$ ) the dissipations are equal

( $U^- = U^+$ ); whereas for  $\alpha \rightarrow 0$  ( $f_{\text{pb}} = 0$ ), Eq. (5) reduces to  $U^+ F^+ = U^- (1 - F^-)$ , which states that for  $\text{Al}^+$  ( $\text{Al}^-$ ) it is solely the hot-electron (hole) dissipation in the Al electrode which affects the detector. In this unrealistic limit, all hot carrier dissipation in the Pb gives rise to phonons which immediately escape to the helium. In Fig. 5 we have used the results of the model calculation in Eq. (5) and a value of  $\alpha = 0.85$  to obtain a set of connectors (dashed lines) which are nearly vertical as a function of current and very much resemble the qualitative features of Fig. 2. The dotted lines at  $V^- = 1.50$  V show the sensitivity of the connectors to the choice of  $\alpha$ .

The plot of Fig. 4 suggests that as a *second hypothesis* we can write for low voltages the linear approximations  $F^+ = 0.5 + \beta V^+$  and  $F^- = 0.5 + \beta V^-$ , where  $\beta$  is a constant depending on barrier parameters. Substituting into Eq. (5), we arrive at the result

$$K = 0.5(U^- - U^+) / (U^- V^- + U^+ V^+) = (1 - \alpha)\beta / (1 + \alpha), \quad (6)$$

where  $K$  is a constant (dimensions of inverse volts) which turns out to be a direct measure of the dissipation asymmetry. This is easily seen by using Eq. (6) in the definitions of the total energy flow fractions to get

$$\begin{aligned} \mathfrak{F}^- &= (f_{\text{Al}} + f_{\text{Pb}})(0.5 - KV^-), \\ \mathfrak{F}^+ &= (f_{\text{Al}} + f_{\text{Pb}})(0.5 + KV^+). \end{aligned} \quad (7)$$

We should note that the asymmetry constant  $K$  can range in value from  $K = 0$  representing symmetric dissipation ( $U^- = U^+$ ) to  $K = \beta$  representing the fully asymmetric case in which only the phonons from the hot carrier dissipation in the Al affect the detector ( $\alpha = 0$  or  $U_{\bar{n}} = U_{\bar{e}}$ ).

## V. DATA ANALYSIS

The constancy of  $K$  ( $\alpha$  and  $\beta$  constant) and hence the validity of our two hypotheses can be checked by inserting the experimentally determined coordinates ( $U, V$ ) of the connector end points into Eq. (6). With the data of Fig. 2, we obtain  $K = 0.111 \pm 0.010(5) V^{-1}$  for the junction without the SiO overlay and  $K^* = 0.0534 \pm 0.0056(5) V^{-1}$  for the same junction with the SiO overlay. The number in parentheses following the standard deviation refers to the number of connectors included in the measurement, and the asterisk (for the purposes of subsequent discussion) refers to the same junction with the SiO overlay. Of course,  $K = 0$  when the He is pumped away leaving a vacuum on the Pb electrode surface.

We have obtained a remarkably similar set of

self-consistent values of  $K$  for a variety of generator-detector configurations out to voltages as large as 1.50 V. For example, three separately evaporated samples similar to that of Fig. 2 gave  $K = 0.113 \pm 0.005(4) V^{-1}$ ,  $K = 0.099 \pm 0.007(6) V^{-1}$ , and  $K = 0.106 \pm 0.008(6) V^{-1}$ . Two additional configurations with a multilayer sandwich  $\text{SiO}(500 \text{ \AA}) - \text{Pb}(7000 \text{ \AA}) - \text{SiO}(500 \text{ \AA})$  separating the generator and detector gave  $K = 0.101 \pm 0.005(6) V^{-1}$  on a glass substrate and  $K = 0.104 \pm 0.003(6) V^{-1}$  on a sapphire substrate. Changing to a sapphire substrate does not appreciably affect  $K$ , but since the thermal conductivity of sapphire is greater than that of glass, more dissipation ( $\sim 2\times$ ) in the generator is required to heat the detector a given amount.

Estimates of relative changes in the fractional ratios  $f_{\text{Al}}/f_{\text{Al}}^*$  and  $f_{\text{Pb}}/f_{\text{Pb}}^*$  can, in principle, be obtained by using a calibrated detector for the dissipation comparisons. In Fig. 2, the triangular points represent those dissipations in the generator junction which cause the maximum conductance at the sum of the gaps in the detector junction (as measured with respect to the normal state conductance) to decrease by a factor of 2. The detector is assumed to have the same absolute sensitivity for both measurements and the bath temperature was held at 1 °K in both cases. For equivalent dissipation in the detector the condition  $\mathfrak{F}^- U^- = \mathfrak{F}^+ U^+ = \mathfrak{F}^* U^{*-} = \mathfrak{F}^{*+} U^{*+}$  must be satisfied. Substituting the coordinates of the connector end points (triangles of Fig. 2) and the experimental values of  $K$  and  $K^*$ , we find

$$\begin{aligned} \frac{f_{\text{Al}} + f_{\text{Pb}}}{f_{\text{Al}}^* + f_{\text{Pb}}^*} &= \frac{(U^{*-}/U^-)(0.5 - V^- K^*)}{0.5 - V^- K} = 0.423 \\ &= \frac{(U^+/U^+)(0.5 + V^+ K^*)}{0.5 + V^+ K} = 0.422 \end{aligned} \quad (8)$$

for negative and positive bias, respectively. This excellent agreement is somewhat fortuitous but does serve as a self-consistency check on the data analysis. The important point to emphasize here is that the SiO layer reduces the effective conductance into the helium to the extent that an experimentally observed factor of  $U^-/U^{*-} = 2.61$  ( $U^+/U^{*+} = 2.22$ ) less dissipation for negative (positive) bias in the generator is required to heat the detector a given amount.

At this point, it is important to consolidate our discussion and emphasize that the origin of the dissipation asymmetry can be traced to two fundamental physical effects. The first effect, as measured by the constant  $\beta$ , is inherent to the tunneling process and reflects the fact that a significant fraction  $F = 0.5 + \beta V$  of the total dissipation can be associated with the hot-electron distribution. The

second effect, as measured by the constant  $\alpha$ , arises because the fraction  $f_{pb}$  of the phonons generated in the Pb electrode that arrives at the detector is less than the corresponding fraction  $f_{Al}$  referred to the Al electrode. The phonon escape probability into the helium is determined by the Kapitza conductance of the Pb-He interface. From the equality  $K = \beta(1 - \alpha)/(1 + \alpha)$  of Eq. (6), it is easily seen that the necessary condition for the realization of our dissipation asymmetry ( $K \neq 0$ ) is that  $\beta \neq 0$  and  $\alpha < 1$ . The tunneling asymmetry characterized by  $\beta$  and the phonon escape asymmetry characterized by  $\alpha$  are insufficient by themselves to produce the observed dissipation asymmetry.

The solid curves of Fig. 6 confirm our physical notations about the trade off between  $\beta$  and  $\alpha$ . These curves were determined by using the experimental values of the asymmetry constants  $K = 0.111 \text{ V}^{-1}$  and  $K^* = 0.0534 \text{ V}^{-1}$ , corresponding to the data of Fig. 2, in combination with Eq. (6) to plot the fraction ratios against the unknown barrier parameter  $\beta$ . The curves of Fig. 6, then, are experimental plots which would uniquely determine the fraction ratios if  $\beta$  could be independently ascertained. If  $\beta$  is large (steep slope in Fig. 4),

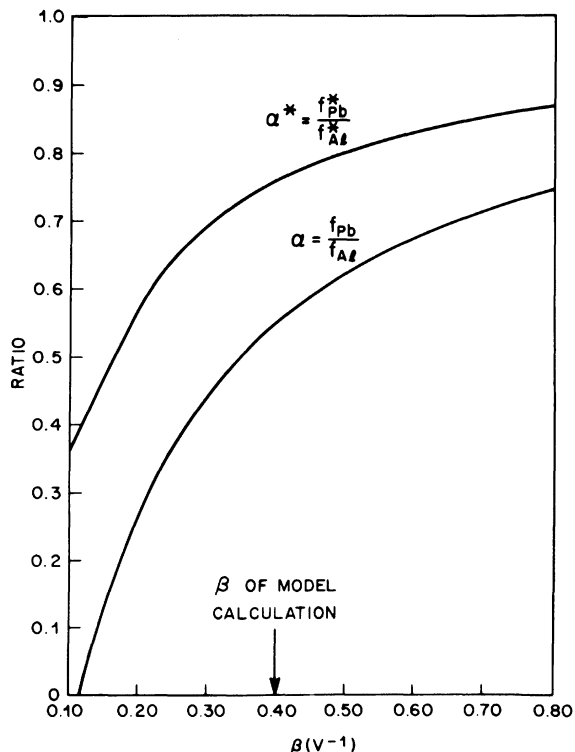


FIG. 6. Plot of fraction ratios ( $\alpha$  and  $\alpha^*$ ) against the unknown barrier parameter  $\beta$ . The curves are based on the experimental determinations of  $K$  and  $K^*$ .

which implies that a significant fraction of energy is dissipated in the hot electron distribution, then the differences between the dissipation fractions  $f_{Pb}$  and  $f_{Al}$  need not be large (i.e.,  $\alpha = f_{Pb}/f_{Al} - 1$ ) in order to produce a given asymmetry. In the opposite small- $\beta$  limit, there would, by necessity, be a large difference between the fractions  $f_{Pb}$  and  $f_{Al}$  ( $\alpha \approx 0$ ) in order to maintain the same dissipation asymmetry as measured by  $K$ . We note from Eq. (6) that all points in Fig. 6 to the left of the minimum  $\beta = K = 0.11 \text{ V}^{-1}$  abscissa (corresponding to  $\alpha = 0$ ) are unphysical. We expect the actual  $\beta$  to be somewhere between this lower limit and the model calculation value of  $\beta = 0.40 \text{ V}^{-1}$ .

## VI. CONCLUDING REMARKS

The discussion of Secs. I-V confirms our physical intuition and tells us that an understanding of the tunneling dissipation asymmetry must involve at least two independent ingredients. Firstly, the relative number of excitations injected into each electrode must be characterized with a description germane to the tunneling process and therefore sensitive to the applied voltage  $V$  and barrier parameters such as  $\phi_1$ ,  $\phi_2$ , and  $d$ . Secondly, the phonon flows to the helium and the substrate must be taken into account. These rely primarily on thermal parameters (Kapitza conductance, interface conductance, etc.), which are appropriate to the materials of the junction and the surrounding environment and are necessarily unrelated to barrier parameters. The physics of these two distinct processes is embodied in the tunneling asymmetry parameter  $\beta$  and the phonon-escape asymmetry parameter  $\alpha$ , respectively. These parameters have been used in combination to derive the asymmetry constant  $K$  of Eq. (6) as a function of the connector end-point measurements ( $U^-$ ,  $V^-$ ,  $U^+$ ,  $V^+$ ). The fact that four independent measurements (two voltages and two currents) are required to specify each connector and that the voltages and currents associated with these connectors vary by almost a factor of 10 for each of six different samples without changing the value of  $K$  by more than 10%, is a strong experimental confirmation of the hypothesis that  $\alpha$  and  $\beta$  are constants independent of the bias voltage. Since the physics seems to require at least a two-parameter theory and the dissipation data are in good agreement with the results of this theory, we therefore conclude that Eqs. (6) and (7) are a highly plausible and possibly unique characterization of the dissipation asymmetry. We have been unable to find an alternative explanation that is consistent with our data.

In using the linear approximation  $F^+ = 0.5 + \beta V^+$  ( $F^- = 0.5 + \beta V^-$ ) to describe the asymmetry in the

electron and hole dissipations, not only have we found that  $\beta$  is a constant but also that it is independent of polarity even for large barrier asymmetry ( $\phi_1 \neq \phi_2$ ). This polarity insensitivity is validated by the data agreement with Eq. (6) and the model calculation results of Fig. 4 for an asymmetric barrier ( $\phi_1 \neq \phi_2$ ). The constant  $\beta$  thus appears to be determined by the average barrier height and is relatively insensitive to barrier-height asymmetries. We therefore conclude that our study of *dissipation asymmetries* cannot provide any further insight into the unsolved problems<sup>7</sup> of *barrier asymmetries* as exemplified in the poor model calculation agreement illustrated in Fig. 3. Even if the Al-I-Pb barrier were completely symmetric ( $\phi_1 = \phi_2$ ), one should still observe dissipation asymmetries; the central difference being that the *connector* end points (Fig. 2) would now lie on different segments of the same polarity independent curve.

As a final remark, it is possible, in principle, to obtain an experimental measure of  $f_{A1} + f_{Pb}$  and hence an absolute determination of  $\mathcal{F}^-$  and  $\mathcal{F}^+$  via Eq. (7). The procedure would be to pump away the liquid helium so that  $U^* = U^{*-} = U^{*+}$  ( $K^* = 0$ ) and  $f_{A1}^* = f_{Pb}^* = 1$ . The asterisk now denotes the absence of liquid helium. The voltages ( $V_0^-$  and  $V_0^+$ ) and dissipations ( $U_0^-$  and  $U_0^+$ ) for an equivalent change in the detector with the helium present would then be measured. These known quantities when substituted into Eq. (8) yield the relation

$$f_{A1} + f_{Pb} = U^* / [U_0^-(0.5 - V_0^-K)] = U^* / [U_0^+(0.5 + V_0^+K)], \quad (9)$$

which when used with Eq. (7) determines the energy flow  $(1 - \mathcal{F}^-)U^-$  or  $(1 - \mathcal{F}^+)U^+$  into helium. This information together with the known temperature dependence of the detector *I-V* characteristics makes it possible to measure directly the Kapitza conductance between the generator junction and the helium. An underlying assumption here is that the phonon bottleneck at the Pb-helium interface is responsible for most of the temperature drop.

In conclusion, we have observed dissipation asymmetries which are inherent to the tunneling process. The asymmetry manifests itself because the phonons generated in the Pb electrode have a greater chance of escaping into the helium than the phonons generated in the Al electrode. The data convincingly confirm some simplifying assumptions about energy flows (constant  $\alpha$ ) and barrier parameters (constant  $\beta$ ) and furthermore suggest a way in which Kapitza conductances can be determined for these thin-film geometries.

#### ACKNOWLEDGMENTS

The author is indebted to R. C. Dynes, T. A. Fulton, and J. M. Rowell for helpful discussions and to P. D. Lazay for the use of his computing facilities. The very competent technical assistance of R. H. Eick in the preparation of the thin-film samples was central to the success of this work.

<sup>1</sup>W. A. Harrison, Phys. Rev. 123, 85 (1961).

<sup>2</sup>J. G. Simmons, J. Appl. Phys. 34, 1793 (1963).

<sup>3</sup>C. B. Duke, *Tunneling in Solids* (Academic, New York, 1969).

<sup>4</sup>R. Stratton, J. Phys. Chem. Solids 23, 1177 (1962).

<sup>5</sup>T. E. Hartman, J. Appl. Phys. 35, 3283 (1964).

<sup>6</sup>J. G. Simmons, J. Appl. Phys. 34, 2581 (1963).

<sup>7</sup>W. F. Brinkman, R. C. Dynes, and J. M. Rowell, J. Appl. Phys. 41, 1915 (1970).

<sup>8</sup>The author is indebted to R. C. Dynes for drawing attention to this process.

<sup>9</sup>S. R. Pollack and C. E. Morris, J. Appl. Phys. 35, 1503 (1964).

<sup>10</sup>K. H. Gundlach and J. Hölzl, Surf. Sci. 27, 125 (1971).

<sup>11</sup>W. Eisenmenger and A. H. Dayem, Phys. Rev. Lett. 18, 125 (1967).

<sup>12</sup>R. C. Dynes, V. Narayanamurti, and M. Chin, Phys. Rev. Lett. 26, 181 (1971).